



University of
Zurich^{UZH}

Zurich Open Repository and
Archive

University of Zurich
Main Library
Strickhofstrasse 39
CH-8057 Zurich
www.zora.uzh.ch

Year: 2019

Spatial variation of human influences on grassland biomass on the Qinghai-Tibetan plateau

Li, Chengxiu ; de Jong, Rogier ; Schmid, Bernhard ; Wulf, Hendrik ; Schaepman, Michael E

Abstract: An improved understanding of increased human influence on ecosystems is needed for predicting ecosystem processes and sustainable ecosystem management. We studied spatial variation of human influence on grassland ecosystems at two scales across the Qinghai-Tibetan Plateau (QTP), where increased human activities may have led to ecosystem degradation. At the 10 km scale, we mapped human-influenced spatial patterns based on a hypothesis that spatial patterns of biomass that could not be attributed to environmental variables were likely correlated to human activities. In part this hypothesis could be supported via a positive correlation between biomass unexplained by environmental variables and livestock density. At the 500 m scale, using distance to settlements within a radius of 8 km as a proxy of human-influence intensity, we found both negatively human-influenced areas where biomass decreased closer to settlements (regions with higher livestock density) and positively human-influenced areas where biomass increased closer to settlements (regions with lower livestock density). These results suggest complex relationships between livestock grazing and biomass, varying between spatial scales and regions. Grazing may boost biomass production across the whole QTP at the 10 km scale. However, overgrazing may reduce it near settlements at the 500 m scale. Our approach of mapping and understanding human influence on ecosystems at different scales could guide pasture management to protect grassland in vulnerable regions on the QTP and beyond.

DOI: <https://doi.org/10.1016/j.scitotenv.2019.01.321>

Posted at the Zurich Open Repository and Archive, University of Zurich

ZORA URL: <https://doi.org/10.5167/uzh-180652>

Journal Article

Accepted Version



The following work is licensed under a Creative Commons: Attribution-NonCommercial-NoDerivatives 4.0 International (CC BY-NC-ND 4.0) License.

Originally published at:

Li, Chengxiu; de Jong, Rogier; Schmid, Bernhard; Wulf, Hendrik; Schaepman, Michael E (2019). Spatial variation of human influences on grassland biomass on the Qinghai-Tibetan plateau. *Science of the Total Environment*, 665:678-689.

DOI: <https://doi.org/10.1016/j.scitotenv.2019.01.321>

Spatial variation of human influences on grassland biomass on the Qinghai-Tibetan Plateau

Chengxiu Li, Rogier de Jong, Bernhard Schmid, Hendrik Wulf and Michael E. Schaepman

Remote Sensing Laboratories, University of Zurich, Winterthurerstrasse 190, CH-8057 Zurich,
Switzerland

* Corresponding author: chengxiu.li@geo.uzh.ch

1 **Abstract:**

2 An improved understanding of increased human influence on ecosystems is needed for
3 predicting ecosystem processes and sustainable ecosystem management. We studied spatial
4 variation of human influence on grassland ecosystems at two scales across the Qinghai-Tibetan
5 Plateau (QTP), where increased human activities may have led to ecosystem degradation. At
6 the 10 km scale, we mapped human-influenced spatial patterns based on a hypothesis that
7 spatial patterns of biomass that could not be attributed to environmental variables were likely
8 correlated to human activities. In part this hypothesis could be supported via a positive
9 correlation between biomass unexplained by environmental variables and livestock density. At
10 the 500 m scale, using distance to settlements within a radius of 8 km as a proxy of human-
11 influence intensity, we found both negatively human-influenced areas where biomass
12 decreased closer to settlements (regions with higher livestock density) and positively human-
13 influenced areas where biomass increased closer to settlements (regions with lower livestock
14 density). These results suggest complex relationships between livestock grazing and biomass,
15 varying between spatial scales and regions. Grazing may boost biomass production across the
16 whole QTP at the 10 km scale. However, overgrazing may reduce it near settlements. Our
17 approach of mapping and understanding human influence on ecosystems at different scales
18 could guide pasture management to protect grassland in vulnerable regions on the QTP and
19 beyond.

20

21 **Keywords** —Alpine grasslands, distance to settlements, human influences, livestock
22 density, overgrazing, remote sensing of biomass, spatial-pattern modeling

23 **1. Introduction**

24 More than three-quarters of the terrestrial biosphere has been altered by human activities

25 (Ellis and Ramankutty, 2008) which has also caused unprecedented changes in many Earth-
26 system processes during the last decades (Chen et al., 2013; Ellis, 2015), including regional
27 and local ecological processes (Ellis and Haff, 2009). It is necessary to understand the
28 consequences of human influence on ecosystems to better explain spatial patterns of
29 ecosystems and their responses to climate and other environmental changes (Ellis, 2015).
30 Ecosystem functioning and services have been most affected in arid and semi-arid areas, where
31 recent degradation has taken place (Chen et al., 2014; Harris, 2010; Wessels et al., 2004). The
32 grassland ecosystems in these areas cover a large portion of the Earth's surface and contain
33 substantial amounts of soil organic carbon. Grassland degradation and land-use changes,
34 including conversion of grassland to cropland, result in a loss of grassland ecosystem carbon
35 stocks (Conant et al., 2017; Guo and Gifford, 2002). This is also the case on the Qinghai-
36 Tibetan Plateau (QTP) (Chen et al., 2013), where vast grassland ecosystems store a large
37 amount of carbon, thus playing a significant role in global carbon cycle (Liu et al., 2016; Ni,
38 2002).

39 The grassland ecosystems on the QTP also influence the local (Xu et al., 2009) and even
40 global climate, e.g. by triggering South Asian monsoon activity (Duan and Wu, 2005). In
41 addition, the QTP is the source region of Asia's major rivers (Figure 1), which supply fresh
42 water for a large part of the world's population downstream (Foggin, 2008; Xu et al., 2008).
43 The stability of ecosystems on the QTP is thus not only of regional importance but also of
44 global relevance for water supply, radiation feedbacks and global climatic patterns (Meyer et
45 al., 2013).

46 The grassland ecosystems on the QTP, characterized by slow plant growth and recovery rate
47 after disturbance (Shang and Long, 2007), are particularly vulnerable to and threatened by
48 pressures from climatic changes and human activities. Degradation of alpine grasslands has
49 indeed been observed on the QTP and led to productivity declines, land desertification and an

50 increase of noxious weeds (Fassnacht et al., 2015; Lehnert et al., 2014a). Such degradation not
51 only damages the livelihoods of local people but also threatens biodiversity and the ecological
52 services of the QTP at large (Harris, 2010). However, the causes of the grassland degradation
53 on the QTP are still unclear and have been related to warming-caused desiccation and
54 permafrost degradation (Harris, 2010; Lehnert et al., 2016) or to increasing human activities
55 (Harris, 2010; P. Wang et al., 2016; Zhaoli et al., 2005).

56 Increasing human activities may have affect grassland biomass production on the QTP,
57 which is mostly covered by rangeland and livestock grazing as the main land-use type (Chen
58 et al., 2013). Privatization of rangeland and semi-nomadic pastoralism have caused increasing
59 grazing pressure (Harris, 2010; Meyer et al., 2013; Wang et al., 2017) and overgrazing of
60 winter pastures (Harris et al., 2016, 2015; L. Li et al., 2017). Moreover, infrastructure
61 development such as highways and townships, tourism and mining exert increasing pressure
62 on QTP grassland ecosystems (S. Li et al., 2017). Human activities of grassland conservation
63 programs (L. Li et al., 2017) and nature reserve programs (S. Li et al., 2018), however, have
64 been launched to protect ecosystems and secure biodiversity and ecosystem services. All these
65 human activities happened at different areas and scales. For example, livestock grazing is
66 widely spread across the whole QTP whereas the grazing pressure is higher in low areas and
67 near settlements. Construction works are site-based and ecosystem protection programs are
68 widely located in the “Three-Rivers headwater regions” in the southern part of Qinghai
69 province. These human activities indicate that human influences on grassland ecosystems are
70 spatially heterogeneous and scale-dependent.

71 The various human activities and land-use intensity on the QTP, combined with clear
72 environmental and productivity gradients (Chen et al., 2015), imply that the grasslands respond
73 differently to diverse human activities on the QTP. For example, the different levels of
74 grassland productivity translate into different carrying capacities for livestock (Miehe et al.,

75 2008), indicating different levels of resistance to grazing and different grazing effects
76 (Milchunas et al., 1988). Previous studies involved quantifying human influence on grassland
77 dynamics (Chen et al., 2014; Lehnert et al., 2016; L. Li et al., 2018) and mapping of human-
78 influence intensity on the QTP (S. Li et al., 2017). However, quantifying and mapping spatially
79 heterogeneous human influence on grassland ecosystems has not been done so far, yet this
80 would be key to understand how ecosystems respond to environmental changes and to help
81 distinguishing climatic and anthropogenic contributions to spatial variation in grassland
82 biomass. We aimed to map human-influenced spatial patterns of grassland biomass on the QTP
83 at two spatial scales, i.e. at the 10 km scale across the whole QTP and at the 500 m scale near
84 human settlements.

85 **2. Data**

86 **2.1 Observed aboveground biomass**

87 Grassland aboveground biomass was assessed using an empirical model based on Landsat-8
88 satellite data and field-measured data (C. Li et al., 2018). Vegetation with higher biomass
89 shows stronger reflectance in near-infrared bands but lower reflectance in visible bands than
90 grassland with lower biomass. The Normalized Difference Vegetation Index (NDVI) was
91 developed to characterize the vegetation (Tucker, 1979) and has been extensively used to
92 estimate aboveground grassland biomass (Jia et al., 2016; Zhang et al., 2016). The 172 biomass
93 plots were measured in the field during peak growing season (late July to mid-August) in 2015
94 and 2016. The closest Landsat-8 NDVI values were extracted with respect to the individual
95 field sampling locations and dates. The field-measured biomass data were randomly split into
96 two parts, using three-quarters of the data for model calibration and one-quarter for validation.
97 The developed empirical model ($R^2 = 0.55$, $rRMSE = 0.23$) was applied to the Landsat-8 NDVI
98 in 2015 to map grassland biomass with the Google Earth Engine (Gorelick et al., 2017) across

99 the whole QTP.

100 We rescaled the aboveground biomass map to a spatial resolution of 10 km and 500 m and
101 further mapped human influences on biomass at 10 km and 500 m scale.

102 **2.2 Climatic variables**

103 The climatic variables used to model the contribution of environmental variables to spatial
104 variation in grassland biomass included growing season (June–September) mean air
105 temperature in 2015 and precipitation in 2015. These variables were extracted from the China
106 Meteorological Forcing Dataset with a spatial resolution of 0.1° (Chen et al., 2011). The
107 temperature variable was constructed by merging observations from 740 meteorological
108 stations and corresponding Princeton meteorological forcing data (Sheffield et al., 2006). The
109 precipitation variable was constructed by combining three precipitation data sets, including
110 observations from the same 740 meteorological stations, the Tropical Rainfall Measuring
111 Mission (TRMM) 3B42 precipitation products (Huffman et al., 2007) and the Asian
112 Precipitation-Highly Resolved Observational Data Integration Towards Evaluation of the
113 Water Resources project (APHRODITE) (Yatagai et al., 2009). This climatic dataset has been
114 widely used in soil moisture modeling and ecosystem studies (Guo and Wang, 2013; Liu and
115 Xie, 2013; Wang et al., 2017).

116 **2.3 Soil properties**

117 Soil variables of soil organic matter, available nitrogen and total phosphorus were selected
118 from eight soil variables (available phosphorus, available potassium, available nitrogen, total
119 phosphorus, total potassium, total nitrogen, soil organic matter and soil PH) to estimate
120 aboveground biomass. The selected soil variables have lowest co-linearity (Variance Inflation
121 Factor <10) with other variables (section 3.2). The soil variables were extracted from a
122 30×30 arcsec resolution gridded soil characteristics dataset (Shangguan et al., 2013). This
123 dataset includes physical and chemical attributes of soils derived from 8979 soil profiles and

124 the Soil Map of China (1:1,000,000). This soil properties dataset has been widely used in soil
125 and ecological studies (Bi et al., 2016; Maire et al., 2015; Sun et al., 2016; Wang et al., 2015).

126 **2.4 Data on eco-geographical regions**

127 The classification of the QTP into eco-geographical regions (Figure 1) was included as a
128 further environmental explanatory variable for spatial variation in grassland biomass (Section
129 3.1). The eco-geographical regions have been defined based on a combination of climatic
130 factors and vegetation types (Gao et al., 2009). We included the classification of eco-
131 geographical regions as an explanatory variable because it reflects the effects of broad
132 differences in species composition between vegetation types on biomass (Chuang et al., 2014).
133 The eco-region data were converted from a polygon-shape file to a raster with 10 km using the
134 statistical software R (R Core Team, 2018).

135 **2.5 Indicators of human influences**

136 Two indicators of human influence, livestock density and distance to settlements, were used
137 to explain the potentially human-influenced spatial patterns at the 10 km and 500 m scale. The
138 settlement locations of cities, towns, hamlets and villages in 2017 were extracted from
139 OpenStreetMap (Haklay and Weber, 2008) as spatial points
140 (<https://download.geofabrik.de/asia/china.html>). The size of settlements was considered when
141 analyzing the correlation between biomass and distance to settlements as described below
142 (section 3.2). The Euclidean distance to the closest of these points was calculated for each grid
143 cell of the QTP (Figure 2).

144 Pasture is the main land-use type on the QTP. Livestock grazing is an important human-
145 influenced activity. Livestock density can serve as an indicator of such human influence.
146 Livestock density was assessed in terms of the number of sheep, goats and yak per square
147 kilometer reported in the 2015 statistical yearbook from Qinghai, Xizang (National Bureau of
148 Statistics of China, 2015). The absolute numbers of different animal species were converted to

149 livestock units using conversion factors of 0.6 for yak and 0.1 for sheep and goats (Lehnert et
150 al., 2016). In the end, livestock densities of 100 counties at the county level were calculated
151 (Figure 2) and decreased from the east to the west of the QTP. The livestock density is suitable
152 to evaluate the human influence on grassland biomass via livestock grazing on the whole QTP
153 scale as demonstrated in previous studies (Lehnert et al., 2016; S. Li et al., 2017). The livestock
154 density data were converted from a polygon shape file to 10 km and 500 m raster in ESRI
155 ArcMap software (<http://desktop.arcgis.com/en/arcmap/>).

156 **3. Methods**

157 **3.1 Model for environmental and human-influenced spatial patterns of biomass at 10** 158 **km scale**

159 We hypothesized that the human-influenced biomass could be calculated from the difference
160 between potential biomass in the absence of human activities and actual biomass estimated
161 from the satellite data. This hypothesis and framework is widely used to quantify human
162 contribution on ecosystem biomass production both at the global scale (Haberl et al., 2014,
163 2007; Krausmann et al., 2013) and at the regional scale of the QTP (Chen et al., 2014; Z. Wang
164 et al., 2016). The potential biomass is the biomass that would be predicted solely by
165 environmental factors without the interference of human activities. Here this potential biomass
166 was defined based on a deterministic empirical model with environmental explanatory
167 variables (x) with regression coefficients β (fixed effects). The actual aboveground biomass,
168 which is influenced by both environmental variables and human activities, was measured from
169 remote sensing NDVI data (y). The difference between potential biomass and actual biomass
170 involves a spatial process (h) that is potentially correlated with human influences (random
171 effects) and a residual noise component ε (Eqn 1) (de Jong et al., 2013). This analysis was
172 conducted at the 10 km scale across the whole QTP by rescaling all environmental explanatory

173 variables to 10 km resolution using the *projectRaster* function in R with bilinear interpolation:

$$174 \quad h = y - x^T \beta - \varepsilon \quad (\text{Eqn 1})$$

175 **a. Deterministic model ($x^T\beta$) attributing biomass to environmental drivers**

176 Temperature, precipitation and soil properties are considered to be the most important
177 variables that may explain spatial biomass variation across the whole QTP (Luo et al., 2004;
178 Sun et al., 2013; Yang et al., 2009). In addition, elevation can account for microclimatic
179 variation and influence grassland biomass (Fisk et al., 1998). Therefore these environmental
180 variables were used to estimate potential biomass.

181 We used each environmental variable's Variance Inflation Factor (VIF) to quantify co-
182 linearity between variables. VIFs are positive values representing the overall correlation of
183 each predictor with all others in a model. Generally, VIF >10 indicate "severe" co-linearity
184 (Neter et al., 1996; Smith et al., 2009). In the end, six environmental variables including
185 temperature, precipitation, available soil nitrogen, total soil phosphorus, soil organic matter,
186 elevation (Table I) and eco-regions (multi-level factor) were used to develop a multiple linear
187 regression model to predict potential biomass. The VIF of selected environmental variables
188 was 2.4 showing low co-linearity.

189 A bootstrapping method was applied when estimating model coefficients to avoid spatial
190 dependency in the training data (de Jong et al., 2013). Five thousand samples were randomly
191 selected from 13574 observations to estimate model coefficients. Three-quarter the samples
192 were used for model calibration and one-quarter of samples were used for model validation.
193 This sampling step was repeated five thousand times to include all data into the model. The
194 relative Root-Mean-Square Errors (rRMSEs (%)), that is the ratio between RMSE and the mean
195 of actual biomass, were averaged to estimate model accuracy. Finally, model coefficients were
196 averaged to estimate environmental-driven biomass at the 10 km scale. In addition, to quantify
197 the relative contribution of each variable to biomass, the relative importance of each

198 environmental variables in the multiple linear regressions was investigated using hierarchical
199 variation partitioning as implemented in the R package *relaimpo* (Grömping, 2006) (Table I).

200 **b. Spatial process (h) and residuals (ε)**

201 We used a Gaussian random field (GRF) to model the spatial patterns of unexplained effects
202 (de Jong et al., 2013). A GRF is described by three elements: 1) a mean function, 2) a range
203 that determines the length scale of the spatial dependency and 3) a sill that determines the
204 marginal variance. The estimated parameter set was used to model the spatial field h . The
205 detailed description of the model can be found in de Jong et al. (2013). Based on our assumption,
206 the modeled spatial patterns are correlated to human activities. We further tested the spatial
207 patterns (h) for correlations with the human-influenced variable livestock density at the county
208 level.

209 The residual component ε contains the remaining spatial variation of biomass that was neither
210 captured by the environmental variables (fixed-effects components fitted in the first step) nor
211 by the spatial process (random-effect components fitted in the second step). In the ideal case,
212 these residuals are spatially uncorrelated (de Jong et al., 2013). This component may contain
213 small-scale human interventions (de Jong et al., 2013; Zhou et al., 2001). To find out whether
214 potential small-scale human interventions could be visible, we also related the residuals to the
215 human-influence variable livestock density (county level).

216 **3.2 Model for human-influenced variation of biomass at the 500 m scale**

217 At the 500 m scale, we used distance to settlements as a proxy of human-influence intensity.
218 Distances to watering points or settlements have been widely used as proxies for grazing
219 intensity in various grassland systems with long pastoral histories (Fernandez-Gimenez and
220 Allen-Diaz, 2001; Manthey and Peper, 2010; Wang et al., 2017). On the QTP, the grazing
221 pressure increased over the past three decades near to the settlements because pasture
222 management was transferred from nomadic to semi-nomadic pastoralism or privatized (Meyer

223 et al., 2013; Wang et al., 2017). Therefore, areas closer to settlements experience more
224 intensive human activities, including higher grazing density, construction work and tourism
225 activities.

226 Human influences on biomass were analyzed within 8-km neighborhoods around settlements
227 at a spatial resolution of 500 m based on previous findings that human influence can be
228 neglected beyond 8 km on the QTP (Liu et al., 2006; Wang et al., 2015). This limit was
229 determined in a breakpoint analysis (see next paragraph). Human activities of grazing,
230 trampling and infrastructure near settlements can directly influence grassland biomass by
231 removal or disturbance, although this may be conterbalanced by compensatory regrowth.
232 Within the range of distances from 0–8 km, a positive correlation between biomass and
233 distance to settlements indicates that biomass is lower near settlements, which suggests a
234 negative human influence on biomass. In contrast, a negative correlation indicates that biomass
235 is higher near settlements, suggesting a positive human influence on biomass. If biomass stays
236 stable along distance to settlements this indicates that human activities do not have a profound
237 influence on biomass. However, beyond the limit distance of 8 km to settlements, the direct
238 human influence on grassland biomass should be small (Liu et al., 2006). Nevertheless,
239 biomass may tend to decrease beyond the limit distance because people avoid areas where
240 potential biomass is low due to harsh environmental conditions (Figure S1). Figure 3 illustrates
241 the above scenarios of changes of biomass along distance to settlements. A supplementary
242 video (supplementary 2) shows examples of changes of biomass along distance to settlements,
243 where a turning point can be observed showing the potential human influential distance and
244 indicating a breakpoint in the relationship between biomass and distance to settlements. The
245 influence of human activities on biomass at the 500 m scale was mapped based on these
246 scenarios.

247 In order to find the specific human influential distance, the *breakpoints* function and *F*

248 statistics test in the R package strucchange were applied (Zeileis et al., 2003), which have been
249 widely used for detecting and monitoring structural changes in (linear) regression models
250 (Zeileis et al., 2003). We configured the algorithm to detect the one most influential breakpoint
251 for each pixel using a moving-window method. We assumed that the maximum human
252 influential distance could be as large as 15 km, according to the 12 km of human influential
253 distance reported from an area in the east of the QTP (Liu et al., 2006). The detected breakpoint
254 distances were averaged across all pixels to get a single estimate for the entire QTP. This
255 yielded the above-mentioned limit distance of 8 km to settlements beyond which direct human
256 influence related to settlements could no longer be detected (Figure 4).

257 To detect the spatial variation of human influence on biomass at the 500 m scale, a moving-
258 window method was applied between distance to settlements and biomass. Specifically, we
259 used local Pearson moving-window regression to show positive and negative influences of
260 human activities on biomass. The selected window size with a radius of 8 km for the local
261 Pearson regression was based on the breakpoint analysis explained above. The area covered by
262 settlements has no biomass value and was therefore excluded from the analysis, that is, human
263 influential distance was calculated to the boundary of a settlement, not an inside point. We
264 finally linked the local Pearson correlation coefficients that represent the human-influenced
265 spatial patterns at the 500 m scale with livestock density. Figure 5 summarizes all data and
266 processing steps as a flowchart.

267 **4. Results**

268 **4.1 Spatial variation in biomass attributed to environmental drivers at the 10 km scale**

269 The biomass data derived from the Landsat-8 NDVI data showed a decreasing gradient from
270 the east to the west of the QTP and additionally varied strongly within the gradient (Figure 6a).
271 The overall spatial variation in biomass across the QTP was decomposed into three parts: 1)

272 variation explained by environmental variables (Figure 6b), 2) variation due to spatial
273 autocorrelation unexplained by environmental variables but potentially correlated with
274 variation in human influences (Figure 6c and Section 4.2) and 3) residual variation neither
275 explained by environmental variables nor by spatial autocorrelation (Figure S2).

276 The model developed from environmental variables including climatic variables, soil
277 properties, topographical variables and eco-regions explained 70% (coefficients of
278 determination $R^2 = 0.70$) of the spatial biomass variation with an accuracy of 27% as measured
279 by the rRMSE. The biomass predicted by these environmental variables clearly showed the
280 decreasing trend towards the west described in the previous paragraph. Among different
281 environmental variables, elevation played the most important role in explaining biomass
282 variation, followed by precipitation and soil available nitrogen (Table I). The relatively lower
283 importance of temperature than elevation was probably due to the higher temperature but low
284 biomass in the Qaidam basin, which was opposite to the general trend of decreasing
285 temperature and biomass along increasing elevation (Figure S5).

286 The biomass predicted by environmental variables shows a sharp transition from high to low
287 biomass along the east-to-west gradient (Figure 6b). This sharp transition was caused by eco-
288 region boundaries and showed the relevance of including eco-regions in the model.

289 **4.2 Spatial variation in biomass potentially due to human-influence at the 10 km scale**

290 The random effects component accounting for spatial autocorrelation in biomass at the 10
291 km scale, which could not be attributed to variation in environmental variables was potentially
292 related to variation in human influences. This spatial autocorrelation component accounts for
293 16% of the spatial variation of biomass. Negative spatial autocorrelations in biomass values
294 occurred on the northern part of Qinghai-lake and in the southern part of the QTP. Positive
295 spatial autocorrelations were mainly found in the eastern part of the QTP (Figure 6c). Both the
296 positive and the negative autocorrelations were clearer in the eastern part of the QTP where

297 human activities are more intense (Figure 2 and Figure 6c). A weak positive correlation ($R^2 =$
298 0.1) was found between the spatial autocorrelation in biomass and the human-influence
299 variable livestock density (Figure 7). No further correlation was found between residuals and
300 livestock density (Figure S3).

301 **4.3 Human-influenced spatial patterns of biomass at the 500 m scale**

302 The influences of human activities on biomass at the 500 m scale were mapped by analyzing
303 biomass along distance to settlements using a moving window radius of 8 km. The map (Figure
304 8) shows both biomass decreases and biomass increases near settlements, indicating positive
305 and negative human influences. Strong negative signals were detected in the Yellow River–
306 Huangshui River Valley and around the southeastern part of Qinghai-lake, Xinghai and Tongde
307 counties (Figure 8 (1)), in the Yarlung Zangbo River valley and in the central Tibetan counties
308 of Doilungdeeqeen, Lasa and Dagze (Figure 8 (3)). In all these areas biomass decreased with
309 proximity to settlements. Positive signals were detected for example in the southeastern part of
310 the QTP, i.e. Baima and Jigzhi counties, where the biomass increased with proximity to
311 settlements (Figure 8 (2)).

312 Across the QTP, positive signals, i.e. higher biomass values closer to settlements, occurred
313 in areas with low livestock density at the 10 km scale. In contrast, the negative signals were
314 correlated with high livestock density, and prevailing negative signals were detected when the
315 regional livestock density was higher than about 22 livestock units per square kilometer (Figure
316 9), even though these regions are also the ones with more productive ecosystems (Figure S4).
317 In general, biomass was actually larger near settlements in areas with low livestock density,
318 whereas biomass was lower near settlements in more productive areas with higher livestock
319 density.

320 **5. Discussion**

321 **5.1 Spatial variation in biomass attributed to environmental drivers at the 10 km scale**

322 The model developed from environmental variables explained most of the spatial
323 variation of biomass (70%). Uncertainties of the model might stem from the limited number of
324 environmental variables used and uncertainties within the environmental variable data, which
325 might affect the potential biomass estimation accuracy. The influence of environmental
326 variables such as soil moisture, soil temperature (X. Wang et al., 2016) and solar radiation
327 (Piao et al., 2006) on biomass has become more important to affect biomass on the QTP under
328 climate change, which should be considered in the future studies. Nevertheless, the
329 environmental variables estimated the potential biomass without the inference of human
330 activities. The difference between the potential biomass and actual biomass are here assumed
331 to be linked with human-influenced variables (Haberl et al., 2007; Pan et al., 2017).

332 **5.2 Human-influenced spatial patterns of biomass at the 10 km scale across the whole**

333 **QTP**

334 A continuing increase in intensity and diversity of human activities exerts spatially
335 heterogeneous influences on grasslands on the QTP. The spatial patterns of human influence
336 on grassland are unknown on the QTP, which are important to understand how different human
337 activities are impacting the ecosystems and how these respond to environmental change. We
338 mapped spatial patterns at two spatial scales and studied whether the patterns can be explained
339 by livestock grazing density.

340 At the 10 km scale, we found that livestock density was positively correlated with the human-
341 influenced spatial pattern of grassland biomass, which indicated that at large scale grazing and
342 biomass have a positive relationship. The QTP has served as pastoral land for thousands of
343 years (Klein et al., 2007; Lu et al., 2017). Grassland ecosystems can become adapted to grazing

344 (Miehe et al., 2009) and major plant species are grazing-resilient (Miehe et al., 2013, 2011).
345 Moderate grazing intensity can promote nutrient recycling and ecosystem production (Lu et al.,
346 2017; Luo et al., 2012). Consistent with these finding, we observed that the potential biomass
347 predicted using only environmental variables was lower than the biomass estimated from the
348 satellite data especially in the eastern part of the QTP, where livestock grazing is the common
349 land use. Appropriate grazing management can affect species composition and facilitate
350 mineral uptake and hydrological processes (Schrama et al., 2013). These effects potentially
351 boost the biomass production, especially in ecosystems that are more productive and more
352 resilient to grazing (Milchunas and Lauenroth, 1993; Wang and Wesche, 2016), which seems
353 to be the case in the eastern and the southeastern part of the QTP (Figure 6c). In summary,
354 positive grazing effects might explain the positive correlation between livestock density and
355 human-influenced spatial patterns in grassland biomass. The opposite causality, i.e. that
356 livestock density is higher where biomass — unexplained by environmental variables — is
357 higher, seems less plausible unless these higher biomass values were caused by unmeasured
358 environmental variables.

359 Except for livestock grazing effects, other human activities including ongoing ecosystem
360 restoration projects and infrastructure development might explain potential human-influenced
361 spatial pattern in grassland biomass (Fig. 6 (b)). This is especially the case in the eastern and
362 central areas of the QTP because in these areas human activities of land-use changes and
363 grazing density are more widespread and more intense (S. Li et al., 2017), whereas in the
364 northwestern part of the QTP human activities are less widespread and less intense (Figure 2).

365 **5.3 Human-influenced spatial patterns of biomass at the 500 m scale**

366 The mobility of pastoralists has decreased and they have become more sedentary across
367 Africa, Asia, the Middle East and the Americas (Sayre et al., 2017), which leads to increased
368 grazing intensity near settlements (Batjargal, 1997; Vanselow et al., 2012). Distance to

369 settlements could potentially serve as a proxy of human-influence intensity in pastoral
370 ecosystems (Fernandez-Gimenez and Allen-Diaz, 2001; Manthey and Peper, 2010), including
371 the QTP (Wang et al., 2017). Thus, recent studies report that livestock-grazing pressure has
372 been increased around settlements on the QTP (Dorji et al., 2013; Hafner et al., 2012; Lehnert
373 et al., 2014b). Here we analyzed how distance to settlements as a proxy of human-influence
374 intensity correlated with grassland biomass across the entire QTP.

375 Increased biomass closer to settlements might suggest positive grazing effects, including
376 effects of increased input of nutrients with cattle manure (Lehnert et al., 2014a). On the other
377 hand, implemented ecosystem restoration projects may also contribute to increased biomass
378 near settlements in some areas, for example in the area of south Sanjiangyuan Jigzhi and Baima
379 County, where positive biomass signals close to settlements were observed (Figure 8 (4) and
380 previous studies of Cai et al., 2015; Xu et al., 2011). However, negative biomass signals close
381 to human settlements were observed in the Xinghai and Tongde County in spite of ecosystem
382 restoration projects in these areas (Figure 8 (1)).

383 Typically, reduced biomass near settlements is taken as an indication of negative human
384 influences due to overgrazing (Hafner et al., 2012). Overgrazing can lead to the reduction of
385 vegetative cover and soil erosion (Papanastasis, 2009; Thornes, 2007), which might be the case
386 in the two regions of the Yarlung Zangbo River valley and the Yellow River-Huangshui River
387 Valley, where we observed negative biomass signals close to human settlements (Figure 8).
388 These regions are characterized by high human population density, livestock-grazing intensity,
389 land use and infrastructure pressure (S. Li et al., 2017). That overgrazing could be one of the
390 main reasons for negative biomass signals near settlements in our study is supported by the fact
391 that these negative signals occurred mainly in areas with high livestock density (Figure 9).

392 The influence of grazing on ecosystem degradation on the QTP is still a topic of debate.
393 Some studies found that heavy grazing causes severe rangeland degradation or even

394 desertification (Song et al., 2009; Wang et al., 2012), whereas other studies found that grazing
395 improved forage quality and extended the growing season (Chen et al., 2013; Harris, 2010;
396 Klein et al., 2007). In the study, we argue that both situations occur on the QTP, depending on
397 the study area and the study scale. Across the whole QTP, grazing is positively related to
398 biomass production at the 10 km scale. However, because of the limited mobility of local
399 herders (Wang et al., 2017), overgrazing occurs near settlements in areas with high livestock
400 density. The overgrazed area might be more vulnerable and more sensitive to climate change,
401 which requires further attention in future ecosystem protection projects.

402 However, the changes of biomass with distance to settlements may also be influenced by
403 other, unmeasured human-influence variables than only by grazing intensity and it may
404 furthermore interact with other environmental variables such as soil properties (Papanastasis,
405 2009). Therefore, the observed spatial patterns need further understanding and validation by
406 combining detailed human activity-indicators with environmental variables. In addition, our
407 study is a single snapshot in time, assessing the human-influenced spatial patterns in grassland
408 biomass in 2015. Future studies should also assess changes over time in these human-
409 influenced spatial patterns.

410 **6. Conclusions**

411 Increased human-influenced activities including livestock grazing and township
412 development exert spatially complex influences on grassland biomass on the QTP. Our study
413 on spatial variation of human influences on grassland biomass on the QTP helps us to
414 understand how these ecosystems may respond to environmental change. At the 10 km scale
415 across the whole QTP we estimated spatial variation of human-influenced biomass by
416 measuring the difference between the potential aboveground biomass without the interference
417 of human activities and actual biomass estimated from the remote sensing data. We found both
418 positive and negative human-influenced spatial patterns across the whole QTP. These patterns

419 positively linked to the livestock density at the county level. At the 500 m scale, we analyzed
420 the human influence on grassland biomass as a function of distance to settlements, used as a
421 proxy of human-influence intensity. This was done because the socioeconomic changes of
422 privatization of pasture land and of sedentarization of nomadic herders was assumed to have
423 increased livestock grazing and other pressures near settlements. We detected hotspots where
424 the biomass decreased or increased towards settlements within a radius of 8 km, indicating
425 both negative and positive human influences on biomass. In particular, we found that biomass
426 decreased near settlements in areas with high livestock density at county level. Overall, our
427 study showed both positive and negative human influences on grassland biomass at two spatial
428 scales, demonstrating the complexity of the relationship between human-influence intensity
429 and grassland biomass, leading to large spatial variation in the relationship across the entire
430 QTP. As a broad generalization we conclude that livestock grazing so far had positive effects
431 on grassland biomass across the whole QTP but overgrazing near settlements now represents
432 a threat to the future biomass production and stability of these ecosystems.

433 **7. Acknowledgements**

434 The forcing climatic dataset used in this study was developed by Data Assimilation and
435 Modeling Center for Tibetan Multi-spheres, Institute of Tibetan Plateau Research, Chinese
436 Academy of Sciences. We acknowledge the OpenStreetMap for providing settlements spatial
437 data. Chengxiu Li was funded by the Chinese Scholarship Council (CSC). This study was
438 conducted in the framework of the University of Zurich Research Program on Global Change
439 and Biodiversity (URPP GCB).

440 **Reference**

- 441 Batjargal, Z., 1997. Desertification in Mongolia. RALA Rep. No. 200 7.
- 442 Cai, H., Yang, X., Xu, X., 2015. Human-induced grassland degradation/restoration in the

443 central Tibetan Plateau: The effects of ecological protection and restoration projects.
444 *Ecol. Eng.* 83, 112–119. doi:10.1016/j.ecoleng.2015.06.031

445 Chen, B., Zhang, X., Tao, J., Wu, J., Wang, J., Shi, P., Zhang, Y., Yu, C., 2014. The impact
446 of climate change and anthropogenic activities on alpine grassland over the Qinghai-
447 Tibet Plateau. *Agric. For. Meteorol.* 189–190, 11–18.
448 doi:10.1016/j.agrformet.2014.01.002

449 Chen, H., Zhu, Q., Peng, C., Wu, N., Wang, Y., Fang, X., Gao, Y., Zhu, D., Yang, G., Tian,
450 J., Kang, X., Piao, S., Ouyang, H., Xiang, W., Luo, Z., Jiang, H., Song, X., Zhang, Y.,
451 Yu, G., Zhao, X., Gong, P., Yao, T., Wu, J., 2013. The impacts of climate change and
452 human activities on biogeochemical cycles on the Qinghai-Tibetan Plateau. *Glob.*
453 *Chang. Biol.* 19, 2940–2955. doi:10.1111/gcb.12277

454 Chen, X., An, S., Inouye, D.W., Schwartz, M.D., 2015. Temperature and snowfall trigger
455 alpine vegetation green-up on the world's roof. *Glob. Chang. Biol.* 21, 3635–3646.
456 doi:10.1111/gcb.12954

457 Chen, Y., Yang, K., He, J., Qin, J., Shi, J., Du, J., He, Q., 2011. Improving land surface
458 temperature modeling for dry land of China. *J. Geophys. Res. Atmos.* 116, 1–15.
459 doi:10.1029/2011JD015921

460 Chuang, L., Ruixiang, S., Wenbo, C., 2014. Eco-regional boundary data of the Roof of the
461 World. *Acta Geogr. Sin.* 69, 140–143. doi:10.3974/Global

462 Conant, R.T., Cerri, C.E.P., Osborne, B.B., Paustian, K., 2017. Grassland management
463 impacts on soil carbon stocks: a new synthesis. *Ecol. Appl.* 27, 662–668.
464 doi:10.1002/eap.1473

465 de Jong, R., Schaepman, M.E., Furrer, R., de Bruin, S., Verburg, P.H., 2013. Spatial
466 relationship between climatologies and changes in global vegetation activity. *Glob.*
467 *Chang. Biol.* 19, 1953–1964. doi:10.1111/gcb.12193

468 Dorji, T., Totland, Ø., Moe, S.R., 2013. Are droppings, distance from pastoralist camps, and
469 pika burrows good proxies for local grazing pressure? *Rangel. Ecol. Manag.* 66, 26–33.
470 doi:10.2111/REM-D-12-00014.1

471 Duan, A.M., Wu, G.X., 2005. Role of the Tibetan Plateau thermal forcing in the summer
472 climate patterns over subtropical Asia. *Clim. Dyn.* 24, 793–807. doi:10.1007/s00382-
473 004-0488-8

474 Ellis, E.C., 2015. Ecology in an anthropogenic biosphere. *Ecol. Monogr.* 85, 287–331.
475 doi:10.1890/14-2274.1

476 Ellis, E.C., Haff, P.K., 2009. Earth science in the anthropocene: New Epoch, new Paradigm,
477 new responsibilities. *Eos (Washington. DC)*. 90, 473. doi:10.1029/2009EO490006

478 Ellis, E.C., Ramankutty, N., 2008. Putting people in the map: Anthropogenic biomes of the
479 world. *Front. Ecol. Environ.* 6, 439–447. doi:10.1890/070062

480 Farr, T., Rosen, P., Caro, E., Crippen, R., Duren, R., Hensley, S., Kobrick, M., Paller, M.,
481 Rodriguez, E., Roth, L., Seal, D., Shaffer, S., Shimada, J., Umland, J., Werner, M.,
482 Oskin, M., Burbank, D., Alsdorf, D., 2007. The shuttle radar topography mission. *Rev.*
483 *Geophys.* 45, 1–33. doi:10.1029/2005RG000183.1.INTRODUCTION

484 Fassnacht, F.E., Li, L., Fritz, A., 2015. Mapping degraded grassland on the Eastern Tibetan
485 Plateau with multi-temporal Landsat 8 data - where do the severely degraded areas
486 occur? *Int. J. Appl. Earth Obs. Geoinf.* 42, 115–127. doi:10.1016/j.jag.2015.06.005

487 Fernandez-Gimenez, M., Allen-Diaz, B., 2001. Vegetation change along gradients from
488 water sources in three grazed Mongolian ecosystems. *Plant Ecol.* 157, 101–118.
489 doi:10.1023/A:1014519206041

490 Fisk, M.C., Schmidt, S.K., Seastedt, T.R., 1998. Topographic patterns of above- and
491 belowground production and nitrogen cycling in alpine tundra. *Ecology* 79, 2253–2266.
492 doi:10.1890/0012-9658(1998)079[2253:TPOAAB]2.0.CO;2

493 Foggin, J.M., 2008. Depopulating the Tibetan Grasslands. *Mt. Res. Dev.* 28, 26–31.
494 doi:10.1659/mrd.0972

495 Gao, J., Li, S., Zhao, Z., 2009. Validating the demarcation of eco-geographical regions: A
496 geostatistical application. *Environ. Earth Sci.* 59, 1327–1336. doi:10.1007/s12665-009-
497 0120-7

498 Gorelick, N., Hancher, M., Dixon, M., Ilyushchenko, S., Thau, D., Moore, R., 2017. Google
499 Earth Engine: Planetary-scale geospatial analysis for everyone. *Remote Sens. Environ.*
500 doi:10.1016/j.rse.2017.06.031

501 Grömping, U., 2006. Relative importance for linear regression in R: the package relaimpo. *J.*
502 *Stat. Softw.* 17, 139–147. doi:10.1016/j.foreco.2006.08.245

503 Guo, D., Wang, H., 2013. Simulation of permafrost and seasonally frozen ground conditions
504 on the Tibetan Plateau, 1981–2010. *J. Geophys. Res. Atmos.* 118, 5216–5230.
505 doi:10.1002/jgrd.50457

506 Guo, L.B., Gifford, R.M., 2002. Soil carbon stocks and land use change: A meta analysis.
507 *Glob. Chang. Biol.* 8, 345–360. doi:10.1046/j.1354-1013.2002.00486.x

508 Haberl, H., Erb, K.-H., Krausmann, F., 2014. Human Appropriation of Net Primary
509 Production: Patterns, Trends, and Planetary Boundaries. *Annu. Rev. Environ. Resour.*
510 39, 363–391. doi:10.1146/annurev-environ-121912-094620

511 Haberl, H., Erb, K.H., Krausmann, F., Gaube, V., Bondeau, A., Plutzer, C., Gingrich, S.,
512 Lucht, W., Fischer-Kowalski, M., 2007. Quantifying and mapping the human
513 appropriation of net primary production in earth’s terrestrial ecosystems. *Proc. Natl.*
514 *Acad. Sci.* 104, 12942–12947. doi:10.1073/pnas.0704243104

515 Hafner, S., Unteregelsbacher, S., Seeber, E., Lena, B., 2012. Effect of grazing on carbon
516 stocks and assimilate partitioning in a Tibetan montane pasture revealed by ¹³C
517 pulse labeling 528–538. doi:10.1111/j.1365-2486.2011.02557.x

518 Haklay, M., Weber, P., 2008. OpenStreet map: User-generated street maps. *IEEE Pervasive*
519 *Comput.* 7, 12–18. doi:10.1109/MPRV.2008.80

520 Harris, R.B., 2010. Rangeland degradation on the Qinghai-Tibetan plateau: A review of the
521 evidence of its magnitude and causes. *J. Arid Environ.* 74, 1–12.
522 doi:10.1016/j.jaridenv.2009.06.014

523 Harris, R.B., Samberg, L.H., Yeh, E.T., Smith, A.T., Wenying, W., Junbang, W., Gaerrang,
524 Bedunah, T.L.D.J., 2016. Rangeland responses to pastoralists' grazing management on a
525 Tibetan steppe grassland, Qinghai Province, China. *Rangel. J.* 38, 1–15.
526 doi:10.1071/RJ15040

527 Harris, R.B., Wenying, W., Badinqiuying, Smith, A.T., Bedunah, D.J., 2015. Herbivory and
528 competition of Tibetan steppe vegetation in winter pasture: Effects of livestock
529 exclosure and plateau pika reduction. *PLoS One* 10. doi:10.1371/journal.pone.0132897

530 Huffman, G.J., Bolvin, D.T., Nelkin, E.J., Wolff, D.B., Adler, R.F., Gu, G., Hong, Y.,
531 Bowman, K.P., Stocker, E.F., 2007. The TRMM Multisatellite Precipitation Analysis
532 (TMPA): Quasi-Global, Multiyear, Combined-Sensor Precipitation Estimates at Fine
533 Scales. *J. Hydrometeorol.* 8, 38–55. doi:10.1175/JHM560.1

534 Jia, W., Liu, M., Yang, Y., He, H., Zhu, X., Yang, F., Yin, C., Xiang, W., 2016. Estimation
535 and uncertainty analyses of grassland biomass in Northern China: Comparison of
536 multiple remote sensing data sources and modeling approaches. *Ecol. Indic.* 60, 1031–
537 1040. doi:10.1016/j.ecolind.2015.09.001

538 Klein, J.A., Harte, J., Zhao, X.Q., 2007. Experimental warming, not grazing, decreases
539 rangeland quality on the Tibetan Plateau. *Ecol. Appl.* 17, 541–557. doi:10.1890/05-0685

540 Krausmann, F., Erb, K.-H., Gingrich, S., Haberl, H., Bondeau, A., Gaube, V., Lauk, C.,
541 Plutzer, C., Searchinger, T.D., 2013. Global human appropriation of net primary
542 production doubled in the 20th century. *Proc. Natl. Acad. Sci.* 110, 10324–10329.

543 doi:10.1073/pnas.1211349110

544 Lehnert, L.W., Meyer, H., Meyer, N., Reudenbach, C., Bendix, J., 2014a. A hyperspectral
545 indicator system for rangeland degradation on the Tibetan Plateau: A case study towards
546 spaceborne monitoring. *Ecol. Indic.* 39, 54–64. doi:10.1016/j.ecolind.2013.12.005

547 Lehnert, L.W., Meyer, H., Meyer, N., Reudenbach, C., Bendix, J., 2014b. A hyperspectral
548 indicator system for rangeland degradation on the Tibetan Plateau: A case study towards
549 spaceborne monitoring. *Ecol. Indic.* 39, 54–64. doi:10.1016/j.ecolind.2013.12.005

550 Lehnert, L.W., Wesche, K., Trachte, K., Reudenbach, C., Bendix, J., 2016. Climate
551 variability rather than overstocking causes recent large scale cover changes of Tibetan
552 pastures. *Sci. Rep.* 6, 24367. doi:10.1038/srep24367

553 Li, C., Wulf, H., Schmid, B., He, J., Schaepman, M.E., Member, S., 2018. Estimating Plant
554 Traits of Alpine Grasslands on the Qinghai-Tibetan Plateau Using Remote Sensing 1–
555 13.

556 Li, L., Fassnacht, F.E., Storch, I., B?rgi, M., 2017. Land-use regime shift triggered the
557 recent degradation of alpine pastures in Nyanpo Yutse of the eastern Qinghai-Tibetan
558 Plateau. *Landsc. Ecol.* 1–17. doi:10.1007/s10980-017-0510-2

559 Li, L., Zhang, Y., Liu, L., Wu, J., Li, S., Zhang, H., Zhang, B., Ding, M., Wang, Z., Paudel,
560 B., 2018. Current challenges in distinguishing climatic and anthropogenic contributions
561 to alpine grassland variation on the Tibetan Plateau. *Ecol. Evol.* 8, 5949–5963.
562 doi:10.1002/ece3.4099

563 Li, S., Wu, J., Gong, J., Li, S., 2018. Human footprint in Tibet: Assessing the spatial layout
564 and effectiveness of nature reserves. *Sci. Total Environ.* 621, 18–29.
565 doi:10.1016/j.scitotenv.2017.11.216

566 Li, S., Zhang, Y., Wang, Z., Li, L., 2017. Mapping human influence intensity in the Tibetan
567 Plateau for conservation of ecological service functions. *Ecosyst. Serv.*

568 doi:10.1016/j.ecoser.2017.10.003

569 Liu, J.G., Xie, Z.H., 2013. Improving simulation of soil moisture in China using a multiple
570 meteorological forcing ensemble approach. *Hydrol. Earth Syst. Sci.* 17, 3355–3369.
571 doi:10.5194/hess-17-3355-2013

572 Liu, L., Zhang, Y., Bai, W., Yan, J., Ding, M., Shen, Z., Li, S., Zheng, D., 2006.
573 Characteristics of grassland degradation and driving forces in the source region of the
574 Yellow River from 1985 to 2000. *J. Geogr. Sci.* 16, 131–142. doi:10.1007/s11442-006-
575 0201-4

576 Liu, S., Zhang, F., Du, Y., Guo, X., Lin, L., Li, Y., Li, Q., Cao, G., 2016. Ecosystem carbon
577 storage in alpine grassland on the Qinghai Plateau. *PLoS One* 11, e0160420.
578 doi:10.1371/journal.pone.0160420

579 Lu, X., Kelsey, K.C., Yan, Y., Sun, J., Wang, X., Cheng, G., Neff, J.C., 2017. Effects of
580 grazing on ecosystem structure and function of alpine grasslands in Qinghai-Tibetan
581 Plateau: A synthesis. *Ecosphere* 8. doi:10.1002/ecs2.1656

582 Luo, G., Han, Q., Zhou, D., Li, L., Chen, X., Li, Y., Hu, Y., Li, B.L., 2012. Moderate grazing
583 can promote aboveground primary production of grassland under water stress 11, 126–
584 136. doi:10.1016/j.ecocom.2012.04.004

585 Luo, T., Pan, Y., Ouyang, H., Shi, P., Luo, J., Yu, Z., Lu, Q., 2004. Leaf area index and net
586 primary productivity along subtropical to alpine gradients in the Tibetan Plateau. *Glob.
587 Ecol. Biogeogr.* 13, 345–358. doi:10.1111/j.1466-822X.2004.00094.x

588 Manthey, M., Peper, J., 2010. Estimation of grazing intensity along grazing gradients - the
589 bias of nonlinearity. *J. Arid Environ.* 74, 1351–1354.
590 doi:10.1016/j.jaridenv.2010.05.007

591 Meyer, H., Lehnert, L.W., Wang, Y., Reudenbach, C., Bendix, J., 2013. Measuring pasture
592 degradation on the Qinghai-Tibet Plateau using hyperspectral dissimilarities and indices.

593 Proc. SPIE 8893, 88931F–88931F–13. doi:10.1117/12.2028762

594 Mieke, G., Mieke, S., Bach, K., Nölling, J., Hanspach, J., Reudenbach, C., Kaiser, K.,
595 Wesche, K., Mosbrugger, V., Yang, Y.P., Ma, Y.M., 2011. Plant communities of central
596 Tibetan pastures in the Alpine Steppe/Kobresia pygmaea ecotone. *J. Arid Environ.* 75,
597 711–723. doi:10.1016/j.jaridenv.2011.03.001

598 Mieke, G., Mieke, S., Bach, K., Wesche, K., Seeber, E., Behrendes, L., Kaiser, K.,
599 Reudenbach, C., Nölling, J., Hanspach, J., Herrmann, M., Yaoming, M., Mosbrugger,
600 V., 2013. Resilience or vulnerability? Vegetation patterns of a Central Tibetan pastoral
601 ecotone. *Steppe Ecosyst. Biol. Divers. Manag. Restor.* 111–151.

602 Mieke, G., Mieke, S., Kaiser, K., Liu, J., Zhao, X., 2008. Status and dynamics of the
603 Kobresia pygmaea ecosystem on the Tibetan plateau. *Ambio* 37, 272–279.
604 doi:10.1579/0044-7447(2008)37[272:SADOTK]2.0.CO;2

605 Mieke, G., Mieke, S., Kaiser, K., Reudenbach, C., Behrendes, L., La Duo, Schlütz, F., 2009.
606 How old is pastoralism in Tibet? An ecological approach to the making of a Tibetan
607 landscape. *Palaeogeogr. Palaeoclimatol. Palaeoecol.* 276, 130–147.
608 doi:10.1016/j.palaeo.2009.03.005

609 Milchunas, D.G., Lauenroth, W.K., 1993. Quantitative effects of grazing on vegetation and
610 soils over a global range of environments. *Ecol. Monogr.* 63, 327–366.
611 doi:10.2307/2937150

612 Milchunas, D.G., Sala, O.E., Lauenroth, W.K., 1988. A Generalized Model of the Effects of
613 Grazing by Large Herbivores on Grassland Community Structure. *Am. Nat.* 132, 87–
614 106.

615 National Bureau of Statistics of China, 2015. *China STATISTICAL YEARBOOK 2015.*
616 China Statistical Press, Beijing.

617 Neter, J., Kutner, M.H., Nachtsheim, C.J., Wasseman, W., 1996. *Applied Linear Statistical*

618 Models, 4th ed. McGraw-Hill.

619 Ni, J., 2002. Carbon storage in grasslands of China. *J. Arid Environ.* 50, 205–218.

620 doi:10.1006/jare.2001.0902

621 Pan, T., Zou, X., Liu, Y., Wu, S., He, G., 2017. Contributions of climatic and non-climatic

622 drivers to grassland variations on the Tibetan Plateau. *Ecol. Eng.* 108, 307–317.

623 doi:10.1016/j.ecoleng.2017.07.039

624 Papanastasis, V.P., 2009. Restoration of degraded grazing lands through grazing

625 management: Can it work? *Restor. Ecol.* 17, 441–445. doi:10.1111/j.1526-

626 100X.2009.00567.x

627 Piao, S., Fang, J., Jinsheng, H.E., 2006. Variations in vegetation net primary production in

628 the Qinghai-Xizang Plateau, China, from 1982 to 1999. *Clim. Change* 74, 253–267.

629 doi:10.1007/s10584-005-6339-8

630 Pugnaire, F.I., Zhang, L., Li, R., Luo, T., 2015. No evidence of facilitation collapse in the

631 Tibetan plateau. *J. Veg. Sci.* 26, 233–242. doi:10.1111/jvs.12233

632 R Core Team, 2018. R: A language and environment for statistical computing. R Found. Stat.

633 Comput. Vienna, Austria.

634 Sayre, N.F., Davis, D.K., Bestelmeyer, B., Williamson, J.C., 2017. Rangelands: Where

635 Anthromes Meet Their Limits. *Land* 6, 31. doi:10.3390/land6020031

636 Schrama, M., Veen, G.F.C., Bakker, E.S.L., Ruifrok, J.L., Bakker, J.P., Olf, H., 2013. An

637 integrated perspective to explain nitrogen mineralization in grazed ecosystems. *Perspect.*

638 *Plant Ecol. Evol. Syst.* 15, 32–44. doi:10.1016/j.ppees.2012.12.001

639 Shang, Z., Long, R., 2007. Formation causes and recovery of the “black Soil Type” degraded

640 alpine grassland in Qinghai-Tibetan Plateau. *Front. Agric. China* 1, 197–202.

641 doi:10.1007/s11703-007-0034-7

642 Shangguan, W., Dai, Y., Liu, B., Zhu, A., Duan, Q., Wu, L., Ji, D., Ye, A., Yuan, H., Zhang,

643 Q., Chen, D., Chen, M., Chu, J., Dou, Y., Guo, J., Li, H., Li, J., Liang, L., Liang, X.,
644 Liu, H., Liu, S., Miao, C., Zhang, Y., 2013. A China data set of soil properties for land
645 surface modeling. *J. Adv. Model. Earth Syst.* 5, 212–224. doi:10.1002/jame.20026

646 Smith, A.C., Koper, N., Francis, C.M., Fahrig, L., 2009. Confronting collinearity: Comparing
647 methods for disentangling the effects of habitat loss and fragmentation. *Landsc. Ecol.*
648 24, 1271–1285. doi:10.1007/s10980-009-9383-3

649 Song, X., Yang, G., Yan, C., Duan, H., Liu, G., Zhu, Y., 2009. Driving forces behind land
650 use and cover change in the Qinghai-Tibetan Plateau: A case study of the source region
651 of the Yellow River, Qinghai Province, China. *Environ. Earth Sci.* 59, 793–801.
652 doi:10.1007/s12665-009-0075-8

653 Sun, J., Cheng, G.W., Li, W.P., 2013. Meta-analysis of relationships between environmental
654 factors and aboveground biomass in the alpine grassland on the Tibetan Plateau.
655 *Biogeosciences* 10, 1707–1715. doi:10.5194/bg-10-1707-2013

656 Thornes, J.B., 2007. Modelling soil erosion by grazing: Recent developments and new
657 approaches. *Geogr. Res.* 45, 13–26. doi:10.1111/j.1745-5871.2007.00426.x

658 Tucker, C.J., 1979. Red and photographic infrared linear combinations for monitoring
659 vegetation. *Remote Sens. Environ.* 8, 127–150. doi:10.1016/0034-4257(79)90013-0

660 Vanselow, K.A., Kraudzun, T., Samimi, C., 2012. Grazing Practices and Pasture Tenure in
661 the Eastern Pamirs. *Mt. Res. Dev.* 32, 324–336. doi:10.1659/MRD-JOURNAL-D-12-
662 00001.1

663 Wang, P., Lassoie, J.P., Morreale, S.J., Dong, S., 2015. A critical review of socioeconomic
664 and natural factors in ecological degradation on the Qinghai-Tibetan Plateau, China.
665 *Rangel. J.* 37, 1–9. doi:10.1071/RJ14094

666 Wang, P., Wolf, S.A., Lassoie, J.P., Poe, G.L., Morreale, S.J., Su, X., Dong, S., 2016.
667 Promise and reality of market-based environmental policy in China: Empirical analyses

668 of the ecological restoration program on the Qinghai-Tibetan Plateau. *Glob. Environ.*
669 *Chang.* 39, 35–44. doi:10.1016/j.gloenvcha.2016.04.004

670 Wang, S., Duan, J., Xu, G., Wang, Y., Zhang, Z., Rui, Y., Luo, C., Xu, B., Zhu, X., Chang,
671 X., Cui, X., Niu, H., Zhao, X., Wang, W., 2012. Effects of warming and grazing on soil
672 N availability, species composition, and ANPP in an alpine meadow. *Ecology* 93, 2365–
673 2376. doi:10.1890/11-1408.1

674 Wang, X., Yi, S., Wu, Q., Yang, K., Ding, Y., 2016. The role of permafrost and soil water in
675 distribution of alpine grassland and its NDVI dynamics on the Qinghai-Tibetan Plateau.
676 *Glob. Planet. Change* 147, 40–53. doi:10.1016/j.gloplacha.2016.10.014

677 Wang, Y., Heberling, G., Görzen, E., Miehe, G., Seeber, E., Wesche, K., 2017. Combined
678 effects of livestock grazing and abiotic environment on vegetation and soils of
679 grasslands across Tibet. *Appl. Veg. Sci.* 20, 327–339. doi:10.1111/avsc.12312

680 Wang, Y., Wesche, K., 2016. Vegetation and soil responses to livestock grazing in Central
681 Asian grasslands: a review of Chinese literature. *Biodivers. Conserv.* 25, 2401–2420.
682 doi:10.1007/s10531-015-1034-1

683 Wang, Z., Zhang, Y., Yang, Y., Zhou, W., Gang, C., Zhang, Y., Li, J., An, R., Wang, K.,
684 Odeh, I., Qi, J., 2016. Quantitative assess the driving forces on the grassland degradation
685 in the Qinghai-Tibet Plateau, in China. *Ecol. Inform.* 33, 32–44.
686 doi:10.1016/j.ecoinf.2016.03.006

687 Wessels, K.J., Prince, S.D., Frost, P.E., Van Zyl, D., 2004. Assessing the effects of human-
688 induced land degradation in the former homelands of northern South Africa with a 1 km
689 AVHRR NDVI time-series. *Remote Sens. Environ.* 91, 47–67.
690 doi:10.1016/j.rse.2004.02.005

691 Xu, J., Grumbine, R.E., Shrestha, A., Eriksson, M., Yang, X., Wang, Y., Wilkes, A., 2009.
692 The melting Himalayas: Cascading effects of climate change on water, biodiversity, and

693 livelihoods. *Conserv. Biol.* 23, 520–530. doi:10.1111/j.1523-1739.2009.01237.x

694 Xu, W., Gu, S., Zhao, X., Xiao, J., Tang, Y., Fang, J., Zhang, J., Jiang, S., 2011. High
695 positive correlation between soil temperature and NDVI from 1982 to 2006 in alpine
696 meadow of the Three-River Source Region on the Qinghai-Tibetan Plateau. *Int. J. Appl.*
697 *Earth Obs. Geoinf.* 13, 528–535. doi:10.1016/j.jag.2011.02.001

698 Xu, X., Lu, C., Shi, X., Gao, S., 2008. World water tower: An atmospheric perspective.
699 *Geophys. Res. Lett.* 35, 1–5. doi:10.1029/2008GL035867

700 Yang, Y.H., Fang, J.Y., Pan, Y.D., Ji, C.J., 2009. Aboveground biomass in Tibetan
701 grasslands. *J. Arid Environ.* 73, 91–95. doi:10.1016/j.jaridenv.2008.09.027

702 Yatagai, A., Arakawa, O., Kamiguchi, K., Kawamoto, H., 2009. A 44-Year Daily Gridded
703 Precipitation Dataset for Asia. *Sola* 5, 3–6. doi:10.2151/sola.2009

704 Zeileis, A., Kleiber, C., Walter, K., Hornik, K., 2003. Testing and dating of structural
705 changes in practice. *Comput. Stat. Data Anal.* 44, 109–123. doi:10.1016/S0167-
706 9473(03)00030-6

707 Zhang, B., Zhang, L., Xie, D., Yin, X., Liu, C., Liu, G., 2016. Application of synthetic NDVI
708 time series blended from landsat and MODIS data for grassland biomass estimation.
709 *Remote Sens.* 8, 10. doi:10.3390/rs8010010

710 Zhaoli, Y., Ning, W., Dorji, Y., Jia, R., 2005. A REVIEW OF RANGELAND
711 PRIVATISATION AND ITS IMPLICATIONS IN THE TIBETAN PLATEAU,
712 CHINA. *Nomad. People.* 9, 31–51.

713 Zhou, L., Tucker, C.J., Kaufmann, R.K., Slayback, D., Shabanov, N. V., Myneni, R.B., 2001.
714 Variations in northern vegetation activity inferred from satellite data of vegetation index
715 during 1981 to 1999. *J. Geophys. Res. Atmos.* 106, 20069–20083.
716 doi:10.1029/2000JD000115

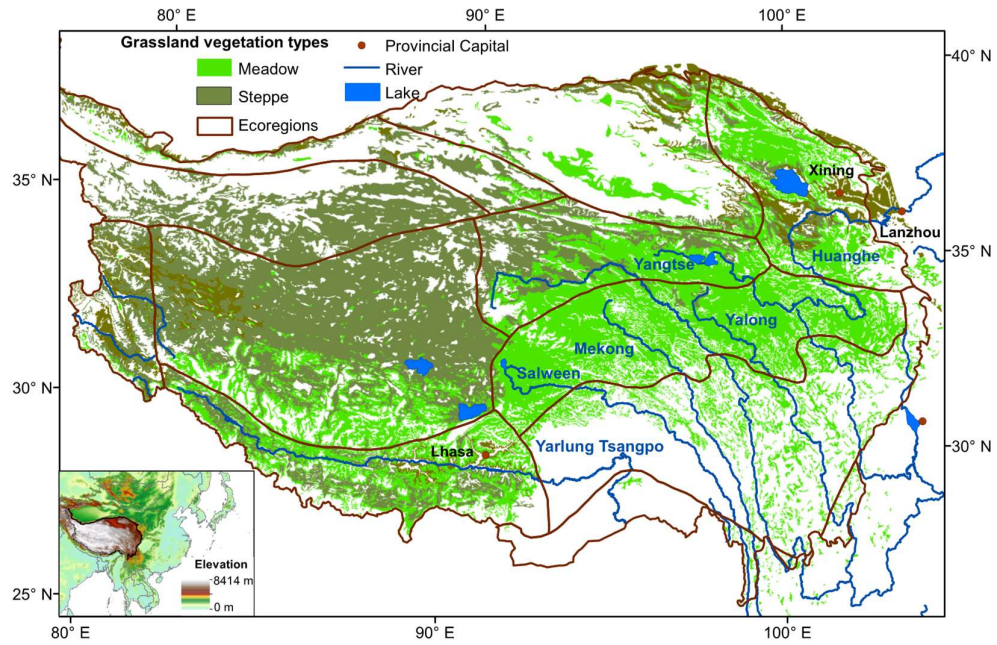
717

718 Table I. Environmental variable's Variance Inflation Factor (VIF) and their relative importance for explaining
719 biomass

Parameter	Unit	VIF	Relative importance
Elevation	m	3.95	0.32
Precipitation	mm	2.59	0.23
Available N	g/100g	2.78	0.23
Soil organic matter	g/100g	2.62	0.13
Temperature	°C	2.30	0.06
Total P	g/100g	1.57	0.03

720

721 Figure 1. Distribution of main grassland vegetation types, eco-regions and major rivers (with names) on the
722 Qinghai-Tibetan Plateau (QTP). Inset indicates elevation data of the extended area based on the NASA Shuttle
723 Radar Topographic Mission (SRTM Version 4; Farr et al., 2007).



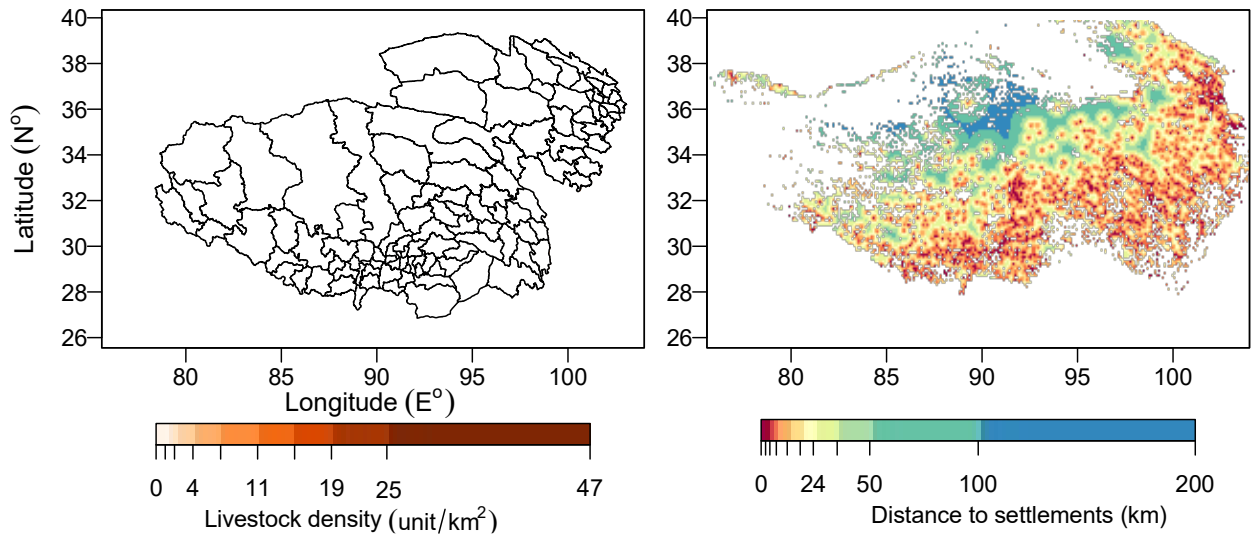
724

725

Figure 2. Livestock density at county level and distance to settlements at the 500 m scale on the Qinghai-

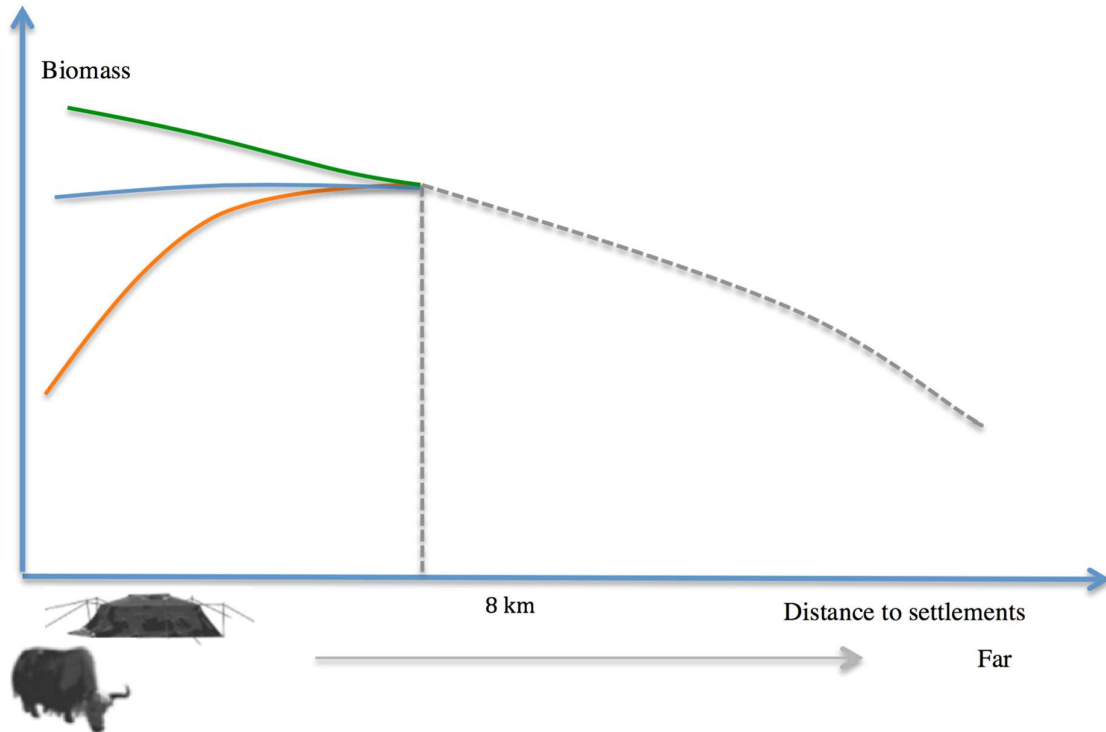
726

Tibetan Plateau.



727

728 Figure 3. Three scenarios of relationships between distance to settlements and grassland biomass: 1 (orange) –
729 biomass decreases near settlements potentially showing a negative human influence on biomass, 2 (blue) – no
730 clear human influence on biomass and 3 (green) – biomass increases near settlements suggesting a positive human
731 influence on biomass. All scenarios hold up to a certain distance (8 km) after which the relationship between
732 biomass and distance tends to be negative (see Figure S1).

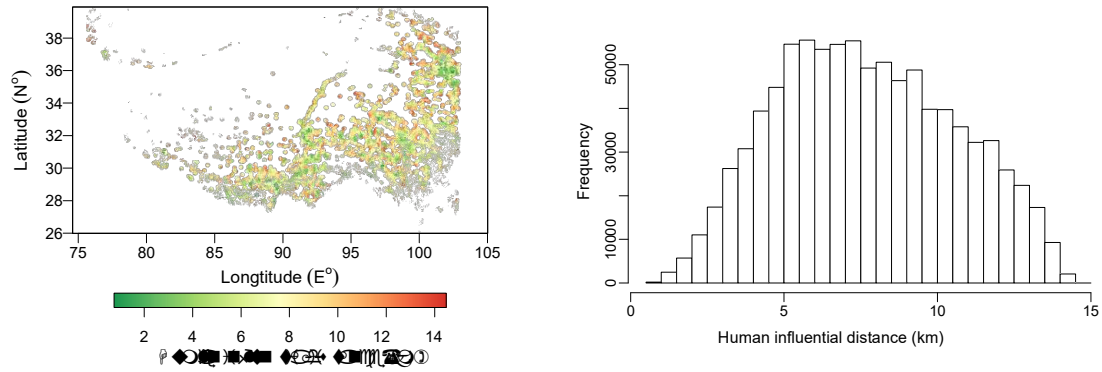


733

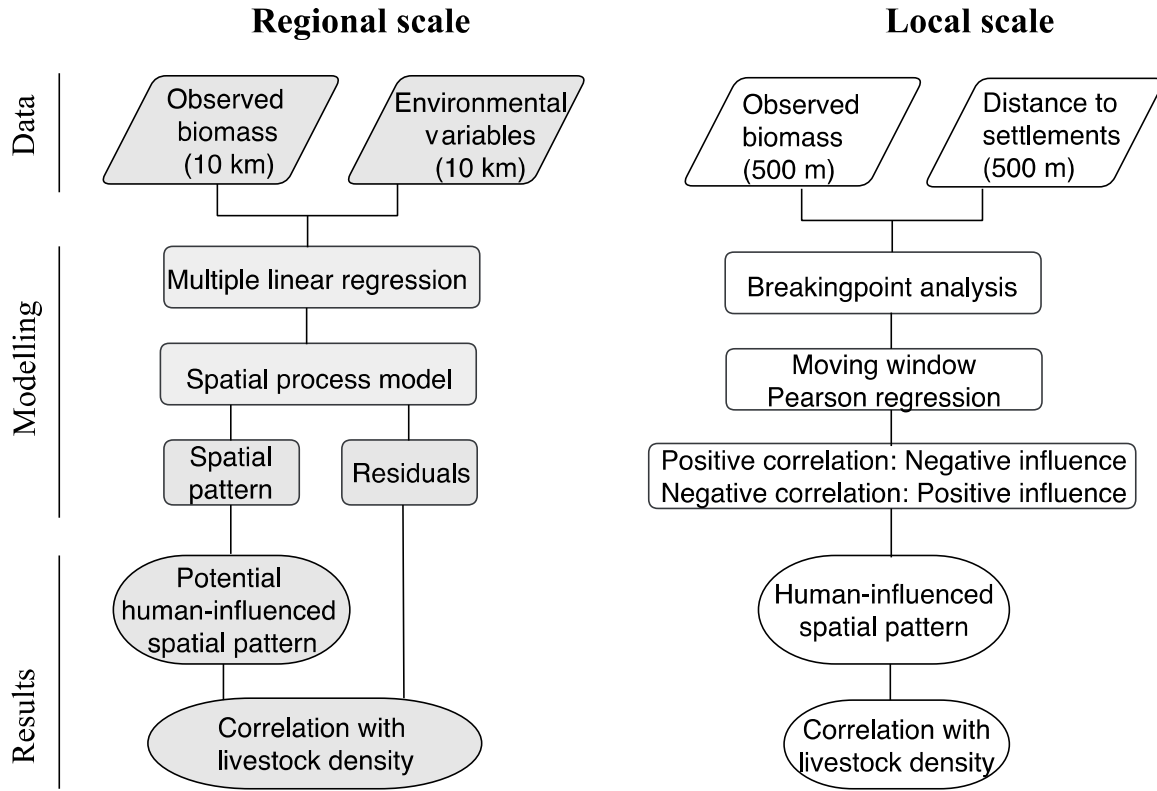
734 Figure 4. The human influential distances on the Qinghai-Tibetan Plateau (a) and their distribution (b).

735 The distances were calculated for local areas using *breakpoints* analysis in R (see Methods). The histogram shows

736 that the average human influential distance is about 8 km.

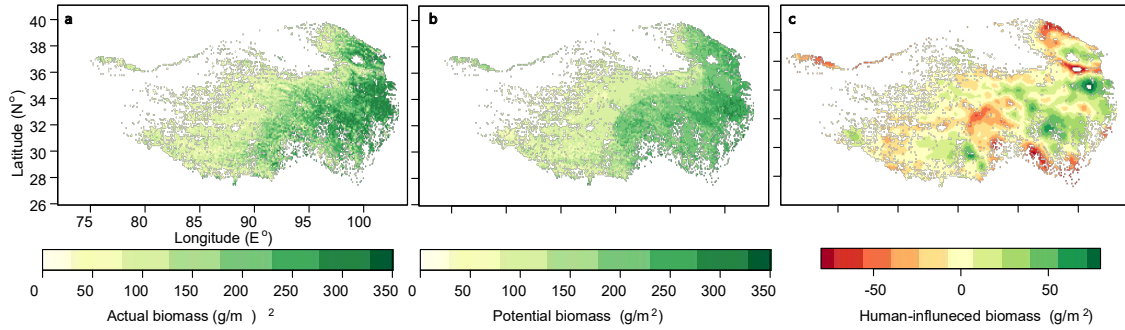


738 Figure 5. Flowchart displaying data and methods used to map the influence of human activities on biomass at 10
 739 km (“Regional”) and 500 m (“Local”) scales.



740

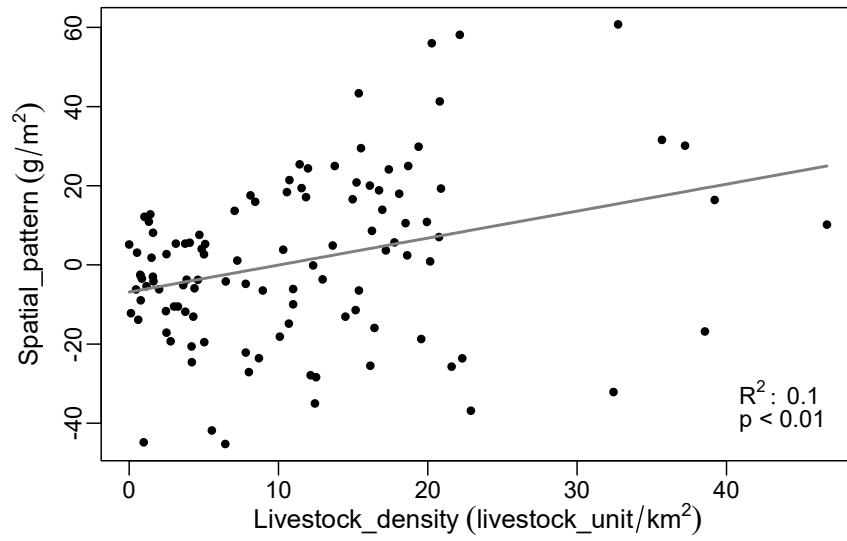
741 Figure 6. Observed biomass using Landsat-8 NDVI vegetation index (a). Biomass predicted using environmental
742 variables (b). Spatial autocorrelation of biomass that could not be explained by environmental variables but
743 possibly human-influence variables (c). Positive hotspots of human influences are indicated with numbers. The
744 circle represents a positive hotspot with a positive human influence at the 500 m scale (Figure 7), whereas the two
745 squares represent positive hotspots with a negative human influence at the 500 m scale.



746

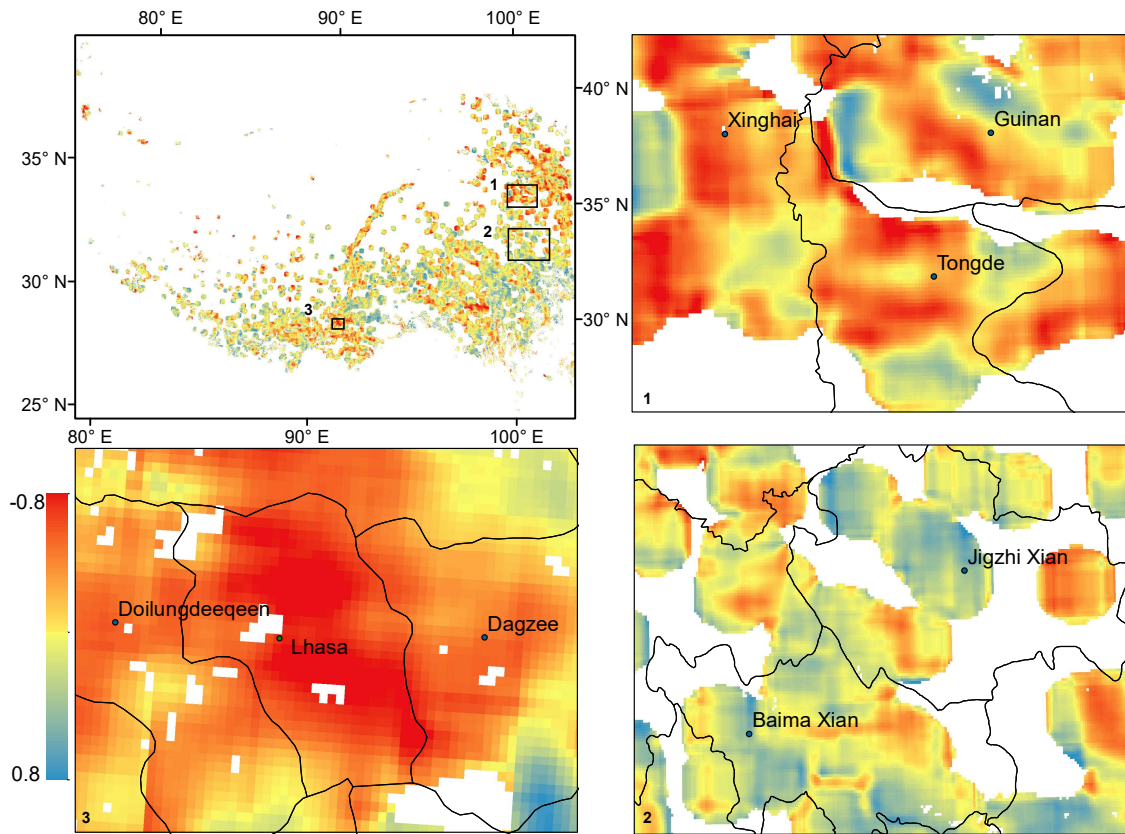
747

748 Figure 7. Scatterplot between human-influenced spatial pattern of grassland biomass (y) and livestock density (x).



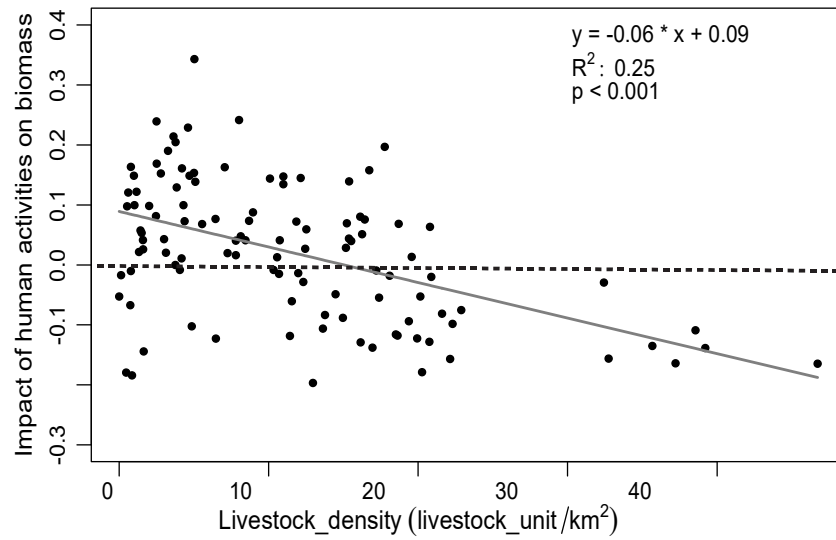
749

750 Figure 8. Correlation coefficients between biomass and distance to settlements (within 8 km) at grid cells of 500
751 m × 500 m (top left panel). A positive correlation shows biomass decreases near settlements and indicates negative
752 human influences and vice versa. Some hotspots of negative and positive human influences area are shown in
753 panels (1), (2), (4).



754

755 Figure 9. Scatterplot between human-influenced spatial biomass pattern at the 500 m scale (y) and livestock
756 density at the 10 km scale (x). Note that a positive human-influenced spatial biomass pattern reflects a negative
757 correlation between local biomass and distance to settlements, i.e. higher biomass close to settlements, and vice
758 versa. The human-influenced spatial biomass pattern was averaged per county and then regressed on the livestock
759 density per county. The dashed line indicates the division between positive and negative human influences on
760 local biomass.



761

762